© 2022. Published by The Company of Biologists Ltd | Development (2022) 149, dev200205. doi:10.1242/dev.200205

RESEARCH ARTICLE

Casein kinase 1α regulates murine spermatogenesis via p53-Sox3 signaling

Chenyang Lu[1,‡], Di Zhang[1,‡], Jinglin Zhang[2,3], Liuhui Li[1], Jingtao Qiu[1,*], Kemian Gou[1,2,4] and Sheng Cui[1,2,4,§]

ABSTRACT

Casein kinase 1α (CK1α), acting as one member of the β-catenin degradation complex, negatively regulates the Wnt/β-catenin signaling pathway. CK1α knockout usually causes both Wnt/β-catenin and p53 activation. Our results demonstrated that conditional disruption of CK1α in spermatogonia impaired spermatogenesis and resulted in male mouse infertility. The progenitor cell population was dramatically decreased in CK1α conditional knockout (cKO) mice, while the proliferation of spermatogonial stem cells (SSCs) was not affected. Furthermore, our molecular analyses identified that CK1α loss was accompanied by nuclear stability of p53 protein in mouse spermatogonia, and dual-luciferase reporter and chromatin immunoprecipitation assays revealed that p53 directly targeted the *Sox3* gene. In addition, the p53 inhibitor pifithrin α (PFTα) partially rescued the phenotype observed in cKO mice. Collectively, our data suggest that CK1α regulates spermatogenesis and male fertility through p53-Sox3 signaling, and they deepen our understanding of the regulatory mechanism underlying the male reproductive system.

KEY WORDS: Casein kinase 1α, Committed progenitor cells, p53, Sox3, Testis

INTRODUCTION

In mammalian spermatogenesis, spermatogonial stem cells (SSCs) produce millions of sperm daily through persistent self-renewal, proliferation (Kanatsu-Shinohara and Shinohara, 2013) and differentiation (Hermann et al., 2015). SSCs are usually recognized as a subpopulation of undifferentiated spermatogonia that are located on the basement membrane of the seminiferous tubules (Tegelenbosch and de Rooij, 1993). The undifferentiated spermatogonia are subdivided into spermatogonial types A_{single} (A_s), A_{paired} (A_{pr}) and $A_{aligned}$ (A_{al}) based on their morphological syncytium length (Phillips et al., 2010). In mice, the traditional SSC model suggests that A_s make up stem cell population, while A_{pr} and A_{al} are committed progenitor cells that do not own self-renewal capabilities (Oakberg, 1971; de Rooij and Russell, 2000). However, advancing studies have demonstrated that undifferentiated spermatogonia (A_s, A_{pr} and A_{al}) are heterogeneous and are distinguished by several genes, such as glial cell line derived neurotrophic factor family receptor α 1 (Gfrα1) and neurogenin 3/SRY-box transcription factor 3 (Ngn3/Sox3) (La and Hobbs, 2019). Ngn3 and Sox3 are expressed by the same subset of A_{al} (McAninch et al., 2020a). Gfrα1$^+$ cells (mainly A_s and A_{pr}, and some A_{al}) are called 'actual stem cells', and Gfrα1$^+$ cells then change into the Ngn3/Sox3$^+$ cells (mainly A_{al} with some A_{pr}), which are referred to as 'potential stem cells', eventually leading to differentiation in steady-state spermatogenesis (Mäkelä and Hobbs, 2019). The transition from Gfrα1$^+$ to Ngn3/Sox3$^+$ spermatogonia indicates that the principal fate of undifferentiated cells will change from self-renewal to differentiation (Suzuki et al., 2009; Nakagawa et al., 2010). Ngn3/Sox3$^+$ committed progenitor cells, which express retinoic acid receptor γ (Rarγ) are regulated by retinoic acid (RA), a factor that promotes differentiation (Wang et al., 2016). Ngn3/Sox3$^+$ committed progenitor cells the differentiate into differentiating spermatogonia (KIT$^+$) before meiosis (Nakagawa et al., 2010).

CK1α is a ubiquitously expressed protein kinase of the serine/threonine protein kinase family (Knippschild et al., 2005a). It has been demonstrated that CK1α exerts its functions by regulating the Wnt/β-catenin pathway (Knippschild et al., 2005b). The Wnt/β-catenin signaling pathway is negatively regulated by CK1α through phosphorylating β-catenin on serine 45; ultimately β-catenin is degraded (Cheong and Virshup, 2011). Moreover, the Wnt/β-catenin pathway is strongly activated and accompanied by p53 signals in CK1α deletion mice, suggesting that CK1α functions in cellular processes by coordinating Wnt with p53 (Elyada et al., 2011). As a transcription factor, p53 has been well documented to function by regulating DNA repair (Williams and Schumacher, 2016), cell cycle progression (Agarwal et al., 1995), programmed cell death (Chen, 2016) and differentiation (Molchadsky et al., 2010). In a steady state, p53 degradation is mediated by murine double minute clone 2 (MDM2) (Coates, 2007) and MDM4 (Wei et al., 2016) to regulate biological processes. In spermatogenesis, the lack of p53 promotes the increase in the early differentiated spermatogonia (Beumer et al., 1998; Xiong et al., 2015). Meanwhile, p53 could be activated by CK1α deletion in many tissues; however, CK1α function and its relation to p53 in mouse testes remains to be clarified.

Our present study provides important insights into the effects of CK1α in spermatogonia. Our results first demonstrate that CK1α is a key factor regulating the biological function of progenitor spermatogonia through the p53/Sox3 signaling pathway, and loss of CK1α results in the decrease of Sox3$^+$ progenitor spermatogonia and male infertility. These results reveal a new mechanism for understanding CK1α function in regulating spermatogenesis and provide a treatment target for male infertility.

[1]College of Veterinary Medicine, Yangzhou University, Yangzhou 225009, Jiangsu, People's Republic of China. [2]Institute of Reproduction and Metabolism, Yangzhou University, Yangzhou 225009, Jiangsu, People's Republic of China. [3]Joint International Research Laboratory of Agriculture and Agri-Product Safety, the Ministry of Education of China, Yangzhou University, Yangzhou 225009, Jiangsu, People's Republic of China. [4]Jiangsu Co-innovation Center for Prevention and Control of Important Animal Infectious Diseases and Zoonoses, Yangzhou 225009, Jiangsu, People's Republic of China.
*Present address: Department of Pathology, Stanford University School of Medicine, Stanford, CA 94305 USA.
‡These authors contributed equally to this work

§Author for correspondence (cuisheng@yzu.edu.cn)

J.Z., 0000-0002-3995-0279; J.Q., 0000-0003-0354-8357; S.C., 0000-0002-3826-3768

Handling Editor: Haruhiko Koseki
Received 16 September 2021; Accepted 31 May 2022

Development (2022) 149, dev200205. doi:10.1242/dev.200205

RESULTS

CK1α expression during mouse testis development

The CK1α mRNA and protein expression levels from postnatal day 1 (P1) to adult (P60) were assayed. The results showed that the *Csnk1a1* mRNA and CK1α protein levels remained at similar levels from P1 to P17, but *Csnk1a1* mRNA sharply increased on P21, which persisted to P35 and P60 (Fig. 1A). Meanwhile, CK1α protein maintained low levels from P1 to P21, which markedly increased on P35 and reached the maximum on P60 (Fig. 1B). We then located CK1α expression in the adult testis by dual immunofluorescence with germ cell marker DEAD box helicase 4 (DDX4) and the Sertoli cell marker WT1. It was observed that nuclear CK1α was expressed in spermatogonia, spermatocytes (Fig. 1C) and Sertoli cells (Fig. 1D). To further confirm the CK1α expression in spermatocytes and spermatids, we detected CK1α expression in mouse testes by dual immunofluorescence with the spermatocyte marker synaptonemal complex protein 3 (Scp3) and the leptotene/zygotene (L/Z) spermatocyte marker DNA meiotic recombinase 1 (Dmc1). These results showed that CK1α was expressed in pachytene/diplotene (P/D) spermatocytes and spermatids instead of L/Z spermatocytes (Figs S1A, S2A).

Furthermore, we assayed the CK1α protein levels using western blot in the germ cells and somatic cells of P7 mouse testes, and the results indicated that the CK1α protein level was significantly higher in the fraction of spermatogenic cells (FSPCs) than in the fraction of somatic cells (FSCs) (Fig. S3A). In addition, we identified the proportions of the CK1α^{+} self-renewing, committed progenitor and spermatogonia cells in P7 mouse testes, which were respectively marked as Gfrα1, Sox3 and PLZF. The results showed that 82.1% self-renewing cells, 87.3% committed progenitor cells and 92.3% spermatogonia were CK1α^{+} (Fig. 1E). Altogether, our data demonstrate that CK1α is expressed in Sertoli cells as well as germ cells, including spermatogonia and P/D spermatocytes and spermatids.

CK1α is essential for male fertility and spermatogenesis

To define the functional role of CK1α in spermatogenesis, the CK1α-conditional knockout mice were established by mating *Stra8-Cre* mice (Sadate-Ngatchou et al., 2008) with *Csnk1a1*^{flox} mice (Elyada et al., 2011) (Fig. 2A). *Stra8-Cre* is first expressed in a subset of undifferentiated spermatogonia from P3 and can be detected up to the preleptotene spermatocyte stage (Zhou et al.,

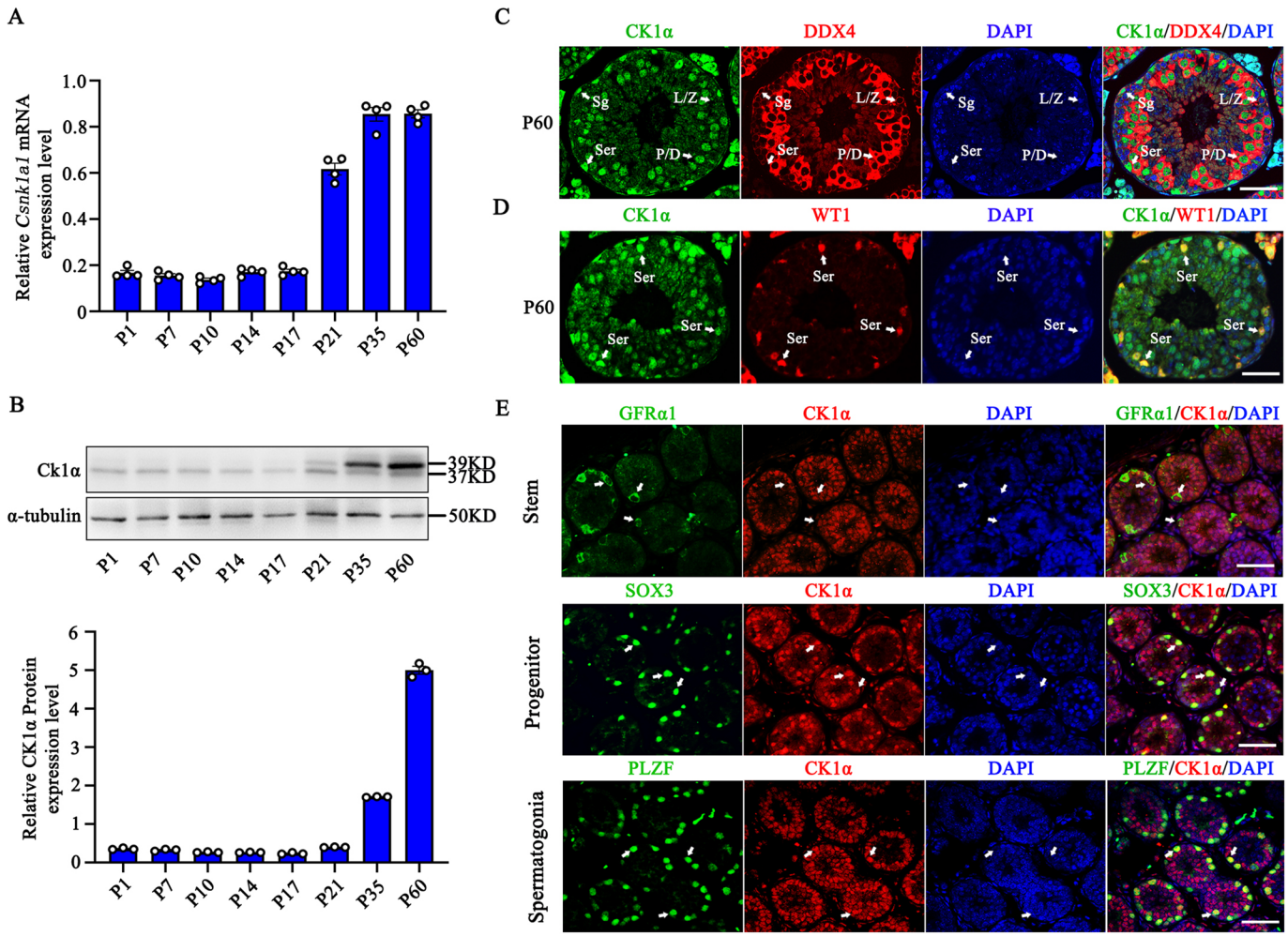

Fig. 1. CK1α is expressed in the mouse testes. (A) Real-time PCR analysis of CK1α expression levels in mouse testes at different stage (n=4). Data are mean±s.e.m. (B) Western blot analysis of CK1α protein levels in mouse testes at different stages (n=3). Data are mean±s.e.m. (C,D) Double-immunofluorescence of P60 seminiferous tubules sections: CK1α (green); DDX4 (red); WT1 (red). Arrows indicate the representative spermatogonia (Sg), leptotene/zygotene spermatocytes (L/Z), pachytene/diplotene spermatocytes (P/D) and Sertoli cells (Ser). Scale bars: 50 µm. (E) Double-immunofluorescence of P7 seminiferous tubules sections: CK1α (red); Gfrα1 (a self-renewing spermatogonia marker, green); Sox3 (a committed progenitor spermatogonia marker, green); PLZF (a total spermatogonia marker, green). Arrows indicate representative CK1α^{+}Gfrα1^{+}, CK1α^{+}Sox3^{+} and CK1α^{+}PLZF^{+} cells. Scale bars: 50 µm.

Development (2022) 149, dev200205. doi:10.1242/dev.200205

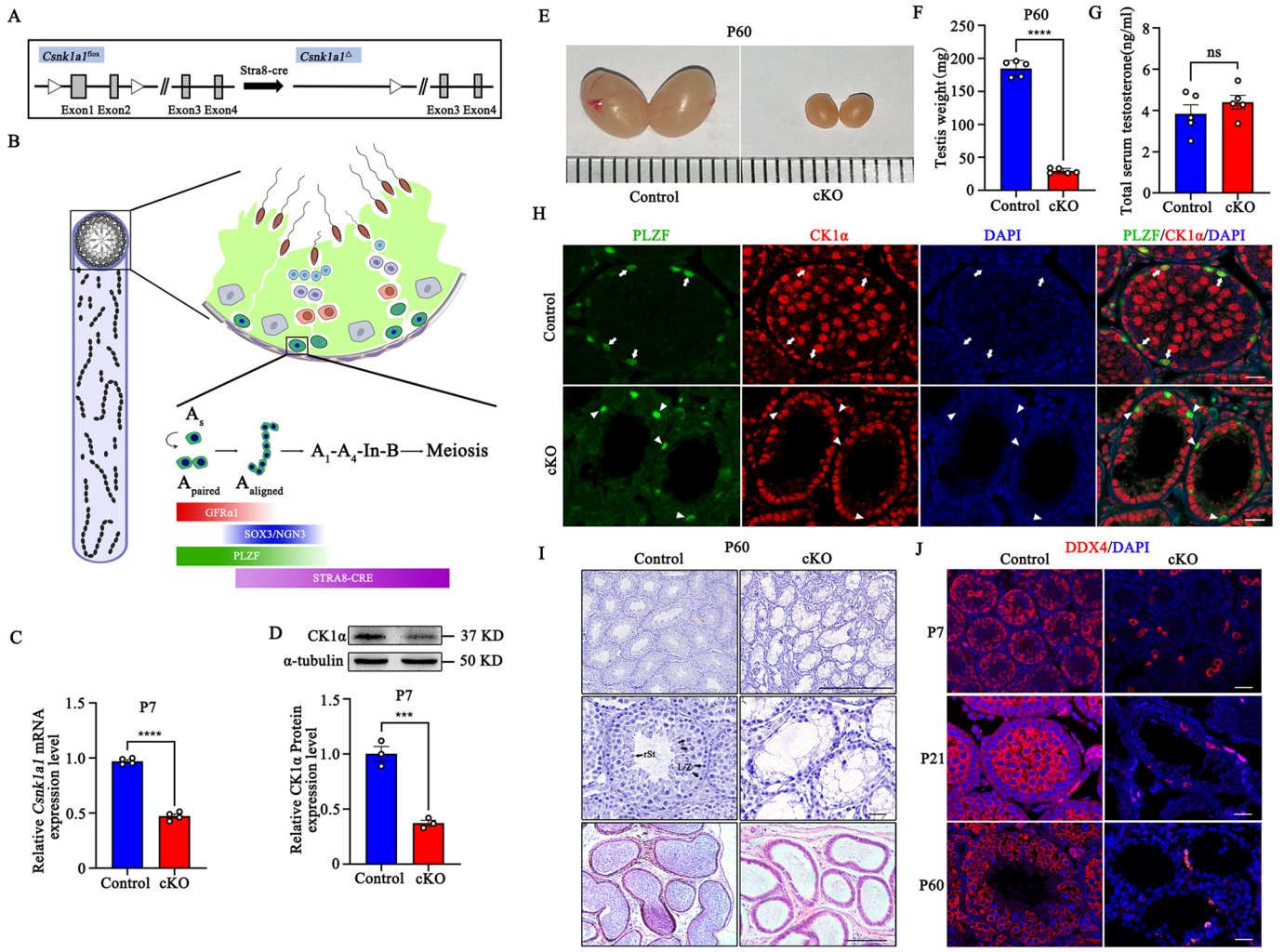

Fig. 2. CK1α is crucial to male fertility and spermatogenesis. (A) Schematic representation of CK1α conditional knockout mouse. (B) Schematic representation of the mouse seminiferous tubule and the *Stra8-cre*-activating time point. (C) Real-time PCR analysis of *Csnk1a1* expression levels in P7 control and cKO testes (n=4, ****P<0.0001). Data are mean±s.e.m. Analysis was determined using an unpaired two-tailed Student's t-test. (D) Western blot analysis of the knockdown efficiency of CK1α protein (n=3, ***P<0.001). Data are mean±s.e.m. Analysis was determined using an unpaired two-tailed Student's t-test. (E) Morphological analysis of P60 control and cKO testes. The ruler scale is divided into 1 mm markers. (F) The testis weight of P60 control and cKO mice (n=5, ****P<0.0001). Data are mean±s.e.m. Analysis was determined using an unpaired two-tailed Student's t-test. (G) Total testosterone concentrations in control and cKO mice serum were assayed by radioimmunoassay (RIA) (n=5; ns, P>0.05). Data are mean±s.e.m. Analysis was determined using an unpaired two-tailed Student's t-test. (H) Double-immunofluorescence staining of CK1α and PLZF in testes of P21 control and cKO mice. Arrows and arrowheads indicate the representative CK1α-positive and -null spermatogonia, respectively. Scale bars: 25 µm. (I) H&E staining of P60 control and cKO testes and caudal epididymis. Scale bars: 50 µm. (J) Immunofluorescence staining of DDX4 (germ cell marker) in testes of P7, P21, P60 control and cKO mice. Scale bars: 50 µm.

2008). It is thus expected to directly knockout CK1α in most of the undifferentiated spermatogonia (Fig. 2B). Real-time PCR and western blot data verified that the mRNA and protein expression of CK1α decreased by 51.3% and 62.6% in P7 mutant testes, respectively (Fig. 2C,D). As CK1α was also expressed in somatic cells, the knockout efficiency was not 100% at the gene and protein levels.

The effects of cKO on body weight and testis size from P7 to P60 were then assayed. The cKO mice were observed to develop normally without significant influence on body weight at every stage examined (Fig. S4A). However, cKO heavily blocked testis growth (Fig. S4B,D), the ratio of cKO testis weight to body weight was lower than that of the controls (Fig. S4C), and the cKO testis weight at P60 was 30 mg, which was one-sixth that of the controls (Fig. 2E,F).

As expected, cKO did not have a significant influence on the serum testosterone level (Fig. 2G). In addition, it was observed that the adult cKO male mice showed typical sex behaviors and were able to mate with the wild-type females, but no mated females became pregnant (Table S1).

Dual immunofluorescence staining revealed that CK1α expression was significantly reduced in PLZF-positive cells in cKO testes, whereas CK1α deletion did not affect CK1α$^+$ Sertoli cells (Fig. 2H, Fig. S5A). To further evaluate *Stra8-Cre*-driven CK1α deletion efficacy in spermatogonia, triple immunofluorescence staining was performed on P7, P14, P21 and P60 testicular sections with antibodies against CK1α, Gfrα1 and Sox3. Our results indicated that the knockout efficiencies of CK1α in Gfrα1$^+$ Sox3$^-$ stem cells were 41.20%, 42.36%, 68.34% and 42.90% in P7, P14, P21 and P60 cKO testes compared with the controls (Fig. S6A,B). Moreover, the expression of CK1α in cKO cultured SSCs was also decreased (Fig. S7A,B). These data confirm that *Stra8-Cre* successfully deletes CK1α from a subset of undifferentiated spermatogonia in the testes of cKO mice.

Development (2022) 149, dev200205. doi:10.1242/dev.200205

Furthermore, P7, P14, P21 and P60 testes were histologically examined by Hematoxylin and Eosin (H&E) staining. It was observed that there were much fewer germ cells and spermatids existed in the cKO testes (Fig. 2I, Fig. S4E). There was also no sperm in the epididymis (Fig. 2I), indicating impaired spermatogenesis in cKO mice. However, no abnormalities were observed in either the testes or epididymis in control mice (Fig. 2I, Fig. S4E). Immunofluorescence results revealed fewer germ cells marked by DDX4 in P7, P21 and P60 cKO testes than in the controls, both in the tubule center and on the basement membrane (Fig. 2J). To further study whether meiosis is completely blocked by CK1α cKO in spermatogonia, the dual immunofluorescence staining of the meiosis marker Scp3 with CK1α was performed on P14 and P21 control and cKO testis sections. The results showed that no spermatocytes were detected in the P14 and P21 cKO mouse testes. Meiosis was completely blocked by CK1α cKO in spermatogonia (Fig. S8). These data confirm that CK1α is crucial to continuous mouse spermatogenesis and the cKO mouse testis defects occur as early as the spermatogonia stage, resulting in infertility.

CK1α deletion decreases the number of Sox3$^+$ progenitor cells

As mentioned above, CK1α knockout beginning from a subset of undifferentiated spermatogonia may influence the biological function of spermatogonia. To identify the time point at which the CK1α knockout resulted in defects in spermatogenesis of spermatogonia, we examined PLZF protein and mRNA expression (in A_s, A_{pr} and A_{al} cells) by western blot and real-time PCR. The results indicated that the PLZF protein levels decreased by 79% and 70% (Fig. 3A) and *PLZF* mRNA decreased by 69% and 73% in P7 and P14 cKO testes, respectively, compared with levels in the controls (Fig. 3B,C). Consistently, there were much fewer PLZF$^+$ cells in the cKO testes than in the controls (Fig. 3D). The cell counting results showed that the average PLZF$^+$ cells numbers were 4.00±0.54 and 3.82±0.42 per the seminiferous tubule cross-section in the P7 and P14 cKO mouse testes, respectively; these were 8.00±0.65 and 10.23±0.56 in the controls (Fig. 3E,F, Tables S4 and S5). Our data demonstrate that CK1α plays crucial roles in the duration of spermatogonia stage.

To investigate whether cKO resulted in the decrease of progenitor spermatogonia, which would be expected to cause a progressive loss of PLZF$^+$ spermatogonia, dual immunofluorescence staining of the progenitor spermatogonia marker Sox3 with PLZF was performed on P7 and P14 cKO testis sections. Sox3 is expressed in the committed progenitor state cells within undifferentiated population spermatogonia and overlaps with Ngn3 expression in mouse testes (Raverot et al., 2005; McAninch et al., 2020b). Statistical results indicated that CK1α deletion resulted in a significant loss of Sox3$^+$ cells in cKO testes (Fig. 3G-J, Tables S6 and S7). Furthermore, the results verified that the *Sox3* mRNA levels decreased by 81% and 87% (Fig. 3B,C), and protein levels decreased by 92% and 83% in P7 and P14 cKO testis, respectively, compared with those in the controls. Together, CK1α deletion results in a decreased number of Sox3$^+$ progenitor cells in the postnatal testes.

CK1α deletion does not affect SSC proliferation and apoptosis

To identify whether CK1α is involved in SSCs functions, we assayed the stem spermatogonia in the control and cKO mouse testes from P7 to P60 using Gfrα1 immunofluorescence staining. The results showed that Gfrα1$^+$ cells were distributed in the basement membrane, and there were no significant differences in the average number of Gfrα1$^+$ cells between the P7, P10, P14 and P21 control and cKO testes per seminiferous tubule cross-section (Fig. 4A,B, Fig. S9A-C,E-G, Table S8-S11). However, the Gfrα1$^+$ stem cells at P60 were accumulated in the basement membrane of seminiferous tubules from cKO testes compared with the controls (Fig. S9D,H, Table S12). These findings suggest that CK1α knockout eventually results in an accumulation of Gfrα1$^+$ cells in adult mouse testes.

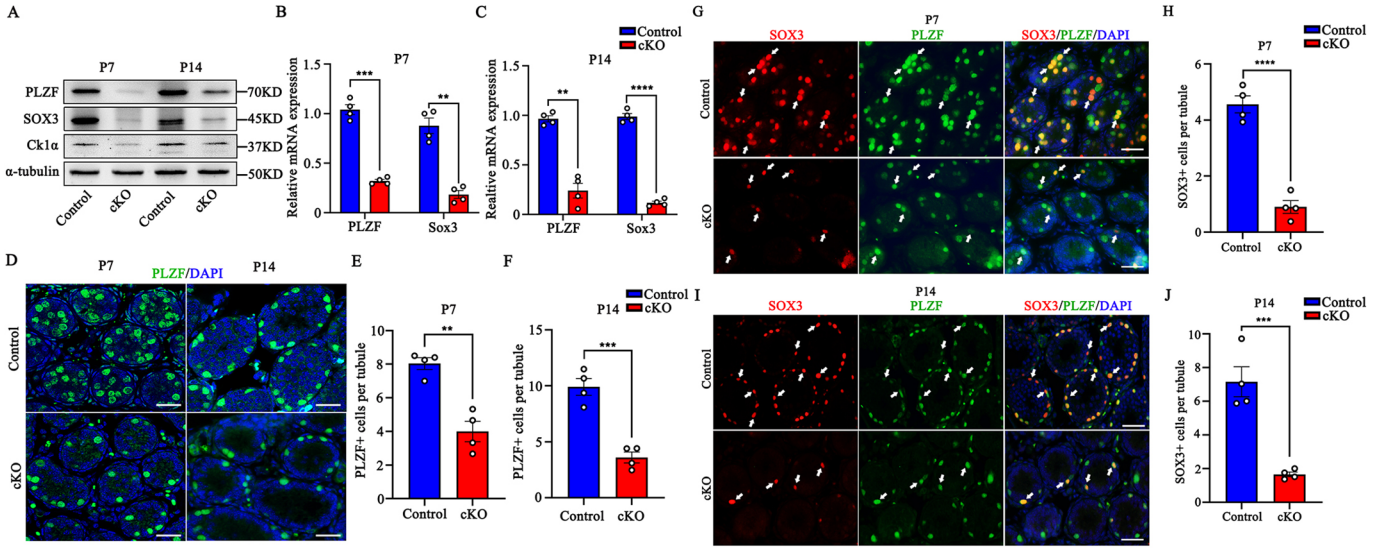

Fig. 3. Sox3$^+$ progenitor spermatogonia are decreased in cKO males. (A) Protein levels of PLZF (spermatogonia marker) and Sox3 (progenitor spermatogonia marker) in P7 and P14 testes of control and cKO mice. (B,C) Expression levels of PLZF and Sox3 were assayed by real-time PCR in P7 (B) and P14 (C) testes of control and cKO mice (n=4, **P<0.01, ***P<0.001, ****P<0.0001). Data are mean±s.e.m. Analyses were determined using an unpaired two-tailed Student's t-test. (D) Immunofluorescence staining of PLZF in P7 and P14 testes of control and cKO mice. Scale bars: 50 µm. (E,F) The numbers of PLZF$^+$ cells per seminiferous tubule in control and cKO testes at P7 (E) and P14 (E) (n=4, **P<0.01, ***P<0.001). Data are mean±s.e.m. Analyses were determined using an unpaired two-tailed Student's t-test. (G,I) Double-immunofluorescence staining of Sox3 and PLZF in P7 and P14 seminiferous tubule sections of control and cKO mice: Sox3 (red); PLZF (green). Scale bars: 50 µm. (H,J) The numbers of Sox3$^+$ cells per seminiferous tubule in control and cKO testes at P7 (H) and P14 (J) (n=4, ***P<0.001, ****P<0.0001). Data are mean±s.e.m. Analyses were determined using an unpaired two-tailed Student's t-test.

Development (2022) 149, dev200205. doi:10.1242/dev.200205

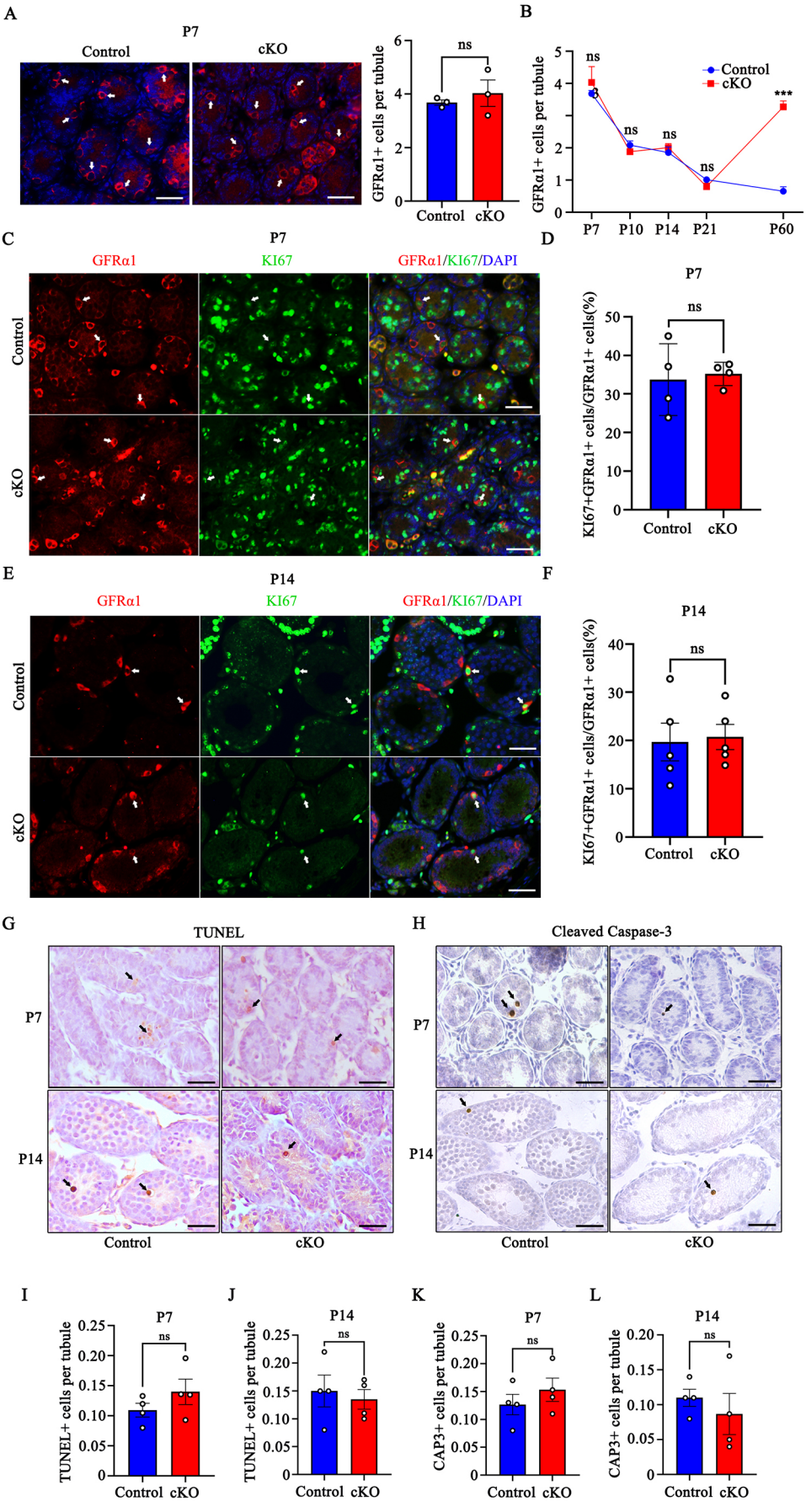

Fig. 4. CK1α knockout did not affect SSC proliferation and apoptosis. (A) Gfrα1 (A_s and A_{pr}) immunofluorescence staining and the numbers of Gfrα1$^+$ cells per seminiferous tubule of control and cKO testes at P7 (*n*=3, ns *P*>0.05). Data are mean±s.e.m. Analysis was determined using an unpaired two-tailed Student's *t*-test. Arrows indicate the representative Gfrα1$^+$ cells. Scale bars: 50 µm. (B) The number of Gfrα1$^+$ cells of control and cKO testes per seminiferous tubule at P7 (*n*=3), P10 (*n*=4), P14 (*n*=4), P21 (*n*=4) and P60 (*n*=4) (ns, *P*>0.05; ***P<0.001). Data are mean±s.e.m. Analyses were determined using an unpaired two-tailed Student's *t*-test. (C,E) Double-immunofluorescence staining of Gfrα1 and Ki67 in control and cKO testes at P7 (C) and P14 (E). Arrows indicate the representative Ki67$^+$ Gfrα1$^+$ cells. Scale bars: 50 µm. (D,F) The ratio of Ki67$^+$ Gfrα1$^+$ cells in Gfrα1$^+$ cells of control and cKO testes at P7 (D) (*n*=4) and P14 (F) (*n*=5) (in %) (ns, *P*>0.05). Data are mean±s.e.m. Analyses were determined using an unpaired two-tailed Student's *t*-test. (G,H) TUNEL and CAP3 staining in control and cKO testes at P7 and P14. Arrows indicate the representative TUNEL$^+$ and CAP3$^+$ cells. Scale bars: 50 µm. (I-L) The numbers of TUNEL$^+$ cells or CAP3$^+$ cells per seminiferous tubule in control and cKO testes at P7 (I,K) and P14 (J,L) (*n*=4, ns *P*>0.05). Data are mean±s.e.m. Analyses were determined using an unpaired two-tailed Student's *t*-test.

Development (2022) 149, dev200205. doi:10.1242/dev.200205

Next, proliferation of Gfrα1$^+$ spermatogonia was assayed by dual staining of Gfrα1 and Ki67 in P7, P14 and P60 testes (Fig. 4C,E, Fig. S10A). The results showed that the proportions of Ki67$^+$ and Gfrα1$^+$ cells were 33.72% ,19.33% and 43.59% in P7, P14 and P60 cKO testes and 34.38%, 20.62% and 45.94% in the control testes, respectively (Fig. 4D,F, Fig. S10B). In addition, cell apoptosis was examined by cleaved caspase 3 (CAP3) immunohistochemistry and TUNEL staining (Fig. 4G,H). Compared with those in controls, no significant differences were detected in the numbers of either CAP3$^+$ or TUNEL$^+$ cells in P7 and P14 cKO testes (Fig. 4I-L, Table S13-16). These data indicate that CK1α knockout has no impact on SSC proliferation and apoptosis.

CK1α deletion increases p53 protein in murine spermatogonia

CK1α regulates biological processes through multiple signaling pathways, including the Wnt/β-catenin and MDM2/p53 pathways. First, we detected whether cKO affected Wnt/β-catenin pathway by western blot. Our data showed that active-β-catenin proteins in P7 and P14 cKO testes were increased by 1.93 times and 1.90 times, and β-catenin proteins were increased 1.26 times and 1.38 times (Fig. S11A,B). In addition, the dual immunofluorescence analysis results showed that some part of the β-catenin signals were transferred from the cytoplasm into the nucleus of spermatogonia (Fig. S11C). These results confirmed that Wnt/β-catenin pathway was activated in cKO mouse testes. However, it has been reported that the Wnt/β-catenin pathway promotes SSC differentiation in order to increase the number of progenitor spermatogonia (Tokue et al., 2017), which was in contrast to our results. To further confirm our results, the cultural SSCs were treated with 20 mM LiCl (a Wnt/β-catenin pathway activator). Real-time PCR results showed that 20 mM LiCl increased *Sox3*, *Ngn3* and *Stra8* mRNA (Fig. S11D). Overall, these results confirm that the Wnt/β-catenin pathway was not the main pathway causing the cKO mouse testes phenotype.

Thus, we speculated that the MDM2/p53 pathway might play a major role in cKO mouse testes. Expectedly, our western blot results showed that MDM2 protein was increased by 1.5 times and p53 protein was increased by 2.3 times in P7 cKO testes, compared with those in controls, while decreased CK1α protein levels were found (Fig. 5A-C). In addition, dual immunofluorescence analysis showed that p53 nuclear signals were detected in cKO testes at P7, while a decrease of CK1α and PLZF was found (Fig. 5D,E).

To further investigate the mechanism of CK1α in spermatogonia, P7 control and cKO testes mRNAs were isolated and RN-sequencing was performed. RNA-sequencing results also revealed upregulation of multiple p53 targeting genes (Fig. 5F). Previous studies have shown that CK1α can regulate p53 stability or activity (Huart et al., 2012), but the molecular mechanism in spermatogonia is unclear. We performed CK1α co-immunoprecipitation from cultured wild-type spermatogonia followed by western blot analysis (Fig. 5G). The data suggest that CK1α interacts with MDM2 and p53 in murine spermatogonia and CK1α knockout results in the increase of p53 protein in murine spermatogonia.

p53 negatively regulates *Sox3* by binding to the *Sox3* promoter

To identify the target genes of p53 to mediate CK1α signaling, we analyzed GO biological processes related to stem cell maintenance

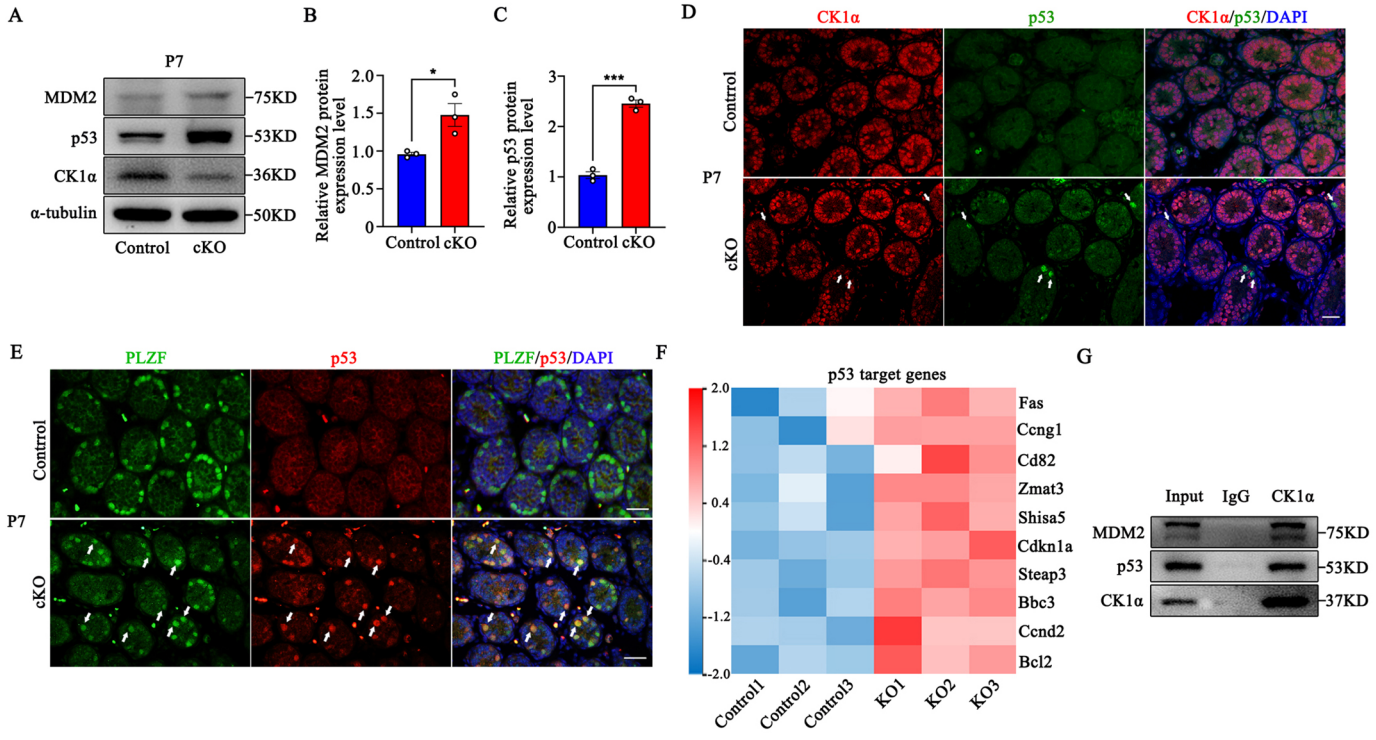

Fig. 5. CK1α deletion resulted in the increase of p53 protein in mouse spermatogonia. (A) Western blot analysis of MDM2, p53 and CK1α protein in P7 control and cKO mouse testes. (B,C) Relative abundances of MDM2 (B) and p53 (C) in P7 control and cKO mouse testes (n=3, *P<0.05, ***P<0.001). Data are mean±s.e.m. Analysis was determined using an unpaired two-tailed Student's t-test. (D) CK1α and p53 double immunofluorescence staining in control and cKO seminiferous tubules sections at P7: p53 (green); CK1α (red). Scale bar: 50 µm. (E) PLZF and p53 double immunofluorescence staining in P7 control and cKO seminiferous tubule sections at P7: PLZF (green); p53 (red). Scale bars: 50 µm. (F) Gene expression of p53 target genes in control and cKO P7 mice shown as a heat map from RNA-seq (n=3). The scale of the heatmap was z-score (row direction) transcripts per kilobase of exon model per million mapped reads. The data are listed in Table S2 (G) CK1α immunoprecipitation in wild-type cultured spermatogonia followed by western blot.

Development (2022) 149, dev200205. doi:10.1242/dev.200205

and stem cell differentiation by RNA-seq (Fig. 6A). Key stem-associated genes (*Itgb1*, *Egr3* and *Cd24a*) were upregulated or unchanged (*Nanos2*, *Cd9*, *Sox2*, *Gfra1*, *Thy1* and *Id4*) (Fig. S12A), whereas levels of *Sox3* (McAninch et al., 2020b), *Ngn3* (Kaucher et al., 2012), *Sohlh1* (Suzuki et al., 2012) and *Sohlh2* (Suzuki et al., 2012), which have been reported to be involved in regulation of progenitor cells, decreased significantly (Fig. 6A). According to these results, *Sohlh1* and *Sohlh2* expression in P7 cKO and control testes was further investigated using *in situ* hybridization. Results demonstrate that *Sohlh1* and *Sohlh2* expression was reduced in P7 cKO testes (Fig. S13A).

Considering that p53, as one of the most well-documented target genes of CK1α, plays a significant role in mouse testes (Xiong et al., 2015), we then performed dual-luciferase reporter assays to investigate whether *Sox3*, *Ngn3*, *Sohlh1* and/or *Sohlh2* were direct target genes of p53. The promoter regions of these genes were cloned and a region 1-2000 bp upstream of the 5′-untranslated regions was selected to explore the relationship between p53 and these genes (Fig. 6B). The assay results demonstrated that p53 overexpression decreased the activity of Sox3-luciferase by 50% but had no significant influence on *Ngn3*-, *Sohlh1*- and *Sohlh2*-luciferase activities (Fig. 6C).

Several putative p53 response elements exist in *Sox3* from −2000 bp to +1 bp from the transcription initiation sites. Chromatin immunoprecipitation (ChIP) was used to assay putative p53 response elements in the mouse Sox3 gene promoter, four areas of which were identified to have putative p53-binding sites (Fig. 6D, Table S19). Four corresponding primer pairs were designed for amplification, and ChIP studies were then performed using p53 antibody. The immunoprecipitated genomic DNA was obtained from P7 control and cKO mouse testes. Of the four putative p53-binding areas, only one region in the −583 bp to −392 bp (P4 region) was occupied by p53 protein (Fig. 6E). Real-time PCR and the fold enrichment method were applied to confirm these results (Fig. 6F,G). To further investigate this in spermatogonia, p53 was activated in the cultured spermatogonial stem cells using the p53 activator nutlin 3 for 24 h. The results showed that 10 µM nutlin 3 decreased *Sox3* mRNA levels by 50% (Fig. 6H). These results confirm that p53 inhibits *Sox3* transcriptional expression by directly binding to the *Sox3* promoter.

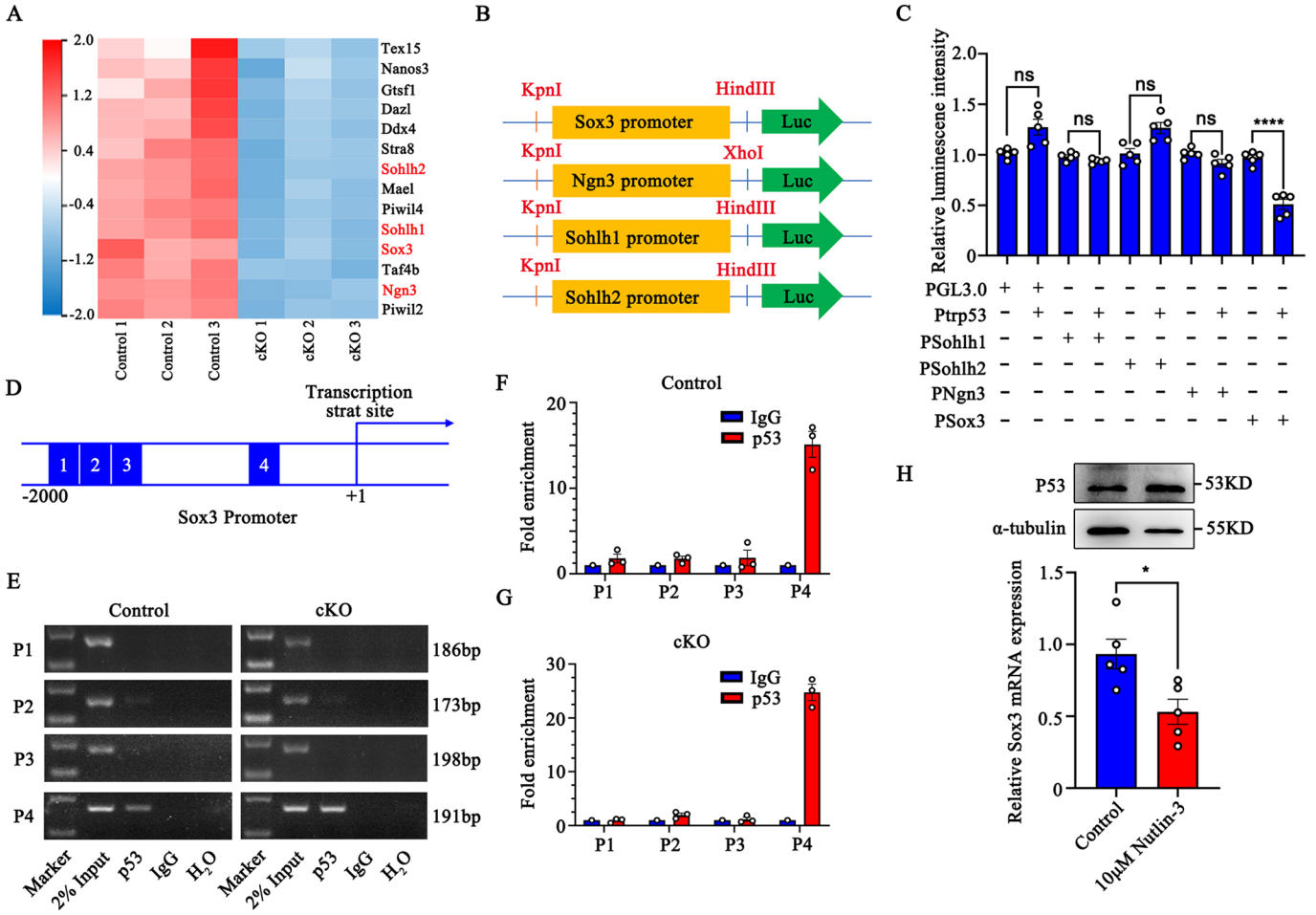

Fig. 6. p53 directly binds to the *Sox3* promoter and negatively regulates *Sox3*. (A) Heatmap showing cell differentiation genes in cKO mice compared with those in control mice. RNA was extracted from P7 testes (n=3). The scale of the heatmap is z-score (row direction) TPM. The data are listed in Table S3. (B) The construction of dual-luciferase reporters of *Sox3*, *Ngn3*, *Sohlh1* and *Sohlh2* promoters. (C) Dual-luciferase reporter assays in response to p53 (n=5; ns, P>0.05; ****P<0.0001). Data are mean±s.e.m. Analyses were determined using an unpaired two-tailed Student's t-test. (D) A schematic representation of the binding sites surrounding the predicted transcription start site of *Sox3*. (E) ChIP-PCR amplification in P7 control and cKO mouse testes using P1-P4 primers. (F,G) Fold change of enriched DNA fragments of P7 control and cKO mouse testes from ChIP detected by real-time PCR analysis. Data are mean±s.e.m. (H) p53 protein levels were assayed by western blot and real-time PCR analysis of *Sox3* mRNA expression in cultured SSCs treated with 10 µM nutlin 3 (n=5, *P<0.05). Data are mean ±s.e.m. Analysis was determined using an unpaired two-tailed Student's t-test.

Development (2022) 149, dev200205. doi:10.1242/dev.200205

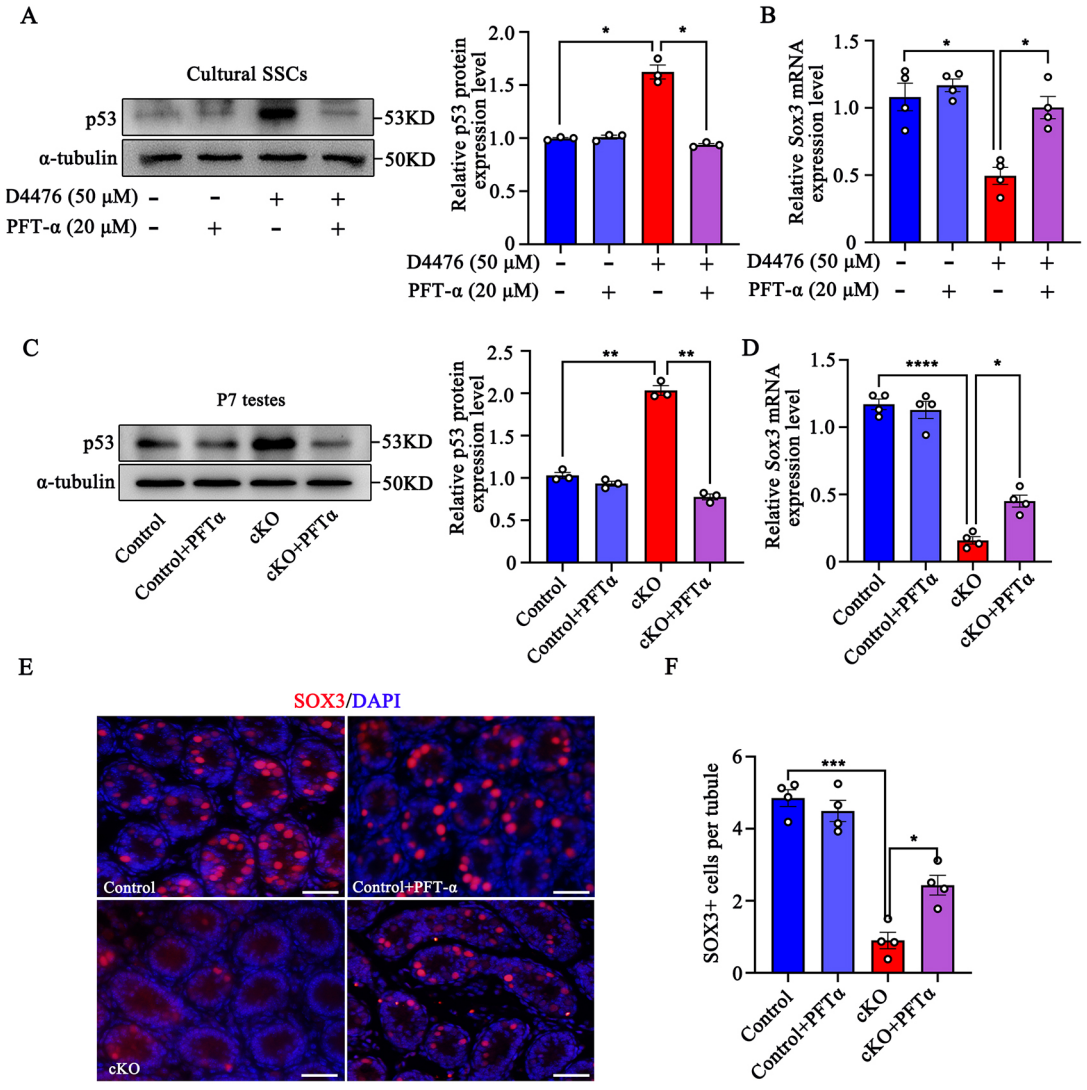

Fig. 7. The inhibition of p53 protein partially restores spermatogenesis in CK1α mutant mice. (A,C) Western blot analysis of p53 protein in cultured SSCs treated with 50 μM D4476 or 20 μM PFTα (A), and in P7 testes injected with 2.2 mg/kg PFTα (C) (n=3, *P<0.05, **P<0.01). Data are mean±s.e.m. Analyses were determined using one-way ANOVA followed by Tukey's multiple comparison test. (B,D) Real-time PCR analysis of Sox3 mRNA in cultured SSCs (B) and P7 testes (D) (n=4, *P<0.05, ****P<0.0001). Data are mean±s.e.m. Analyses were determined using one-way ANOVA followed by Tukey's multiple comparison test. (E) Immunofluorescence staining of Sox3 in P7 control and cKO testes with injection of NaCl and PFTα. Scale bars: 50 μm. (F) The number of Sox3$^+$ progenitor cells per seminiferous tubule in P7 control and cKO testes with or without PFTα (n=4, *P<0.05, ***P<0.001). Data are mean±s.e.m. Analysis was determined using one-way ANOVA followed by Tukey's multiple comparison test.

p53 inhibition partially restores spermatogenesis in CK1α mutant mice

If regulation of p53 levels by CK1α greatly influences the biological function of progenitor cells in mouse testes, we expected that regulation of p53 levels may rescue the cKO mouse phenotypes. To confirm this, the cultured mouse SSCs were treated with 20 μM p53 inhibitor pifithrin α (PFTα) for 1 h and then treated with 50 μM CK1α inhibitor D4476 for 24 h. Western blot results showed that PFTα treatment successfully inhibited the enhancing effect of D4476 on p53 protein expression from 1.68-fold to 0.92-fold (Fig. 7A). The *Sox3* mRNA level in the harvested cells was assayed by real-time PCR, which revealed that PFTα restored from 42.8% to 86.9% the *Sox3* mRNA expression that was downregulated by D4476 (Fig. 7B).

We further tried to determine whether inhibiting p53 could rescue the cKO testis phenotypes by injecting PFTα (2.2 mg/kg) intraperitoneally into control and cKO mice every day from P3 until P7. The western blot results showed that PFTα successfully decreased the p53 protein level from 2.07-fold to 0.88-fold in P7 cKO testes (Fig. 7C), and the *Sox3* mRNA levels recovered significantly from 15.7% to 41.8% compared with levels in the controls (Fig. 7D). Consistently, the suppression of p53 protein led to an increase in Sox3$^+$ cell numbers from 0.90±0.23 to 2.44±0.88 in P7 cKO testes (Fig. 7E,F). In conclusion, CK1α is involved in murine testis development and spermatogenesis by regulating the p53-Sox3 signaling pathway.

DISCUSSION

CK1α has been reported to play important roles in various biological processes; however, its function in spermatogenesis is poorly understood. In our study, we demonstrate that CK1α functions in committed progenitor spermatogonia through the p53/Sox3 signaling pathway (Fig. 8).

The results presented here demonstrate that CK1α deletion inhibits spermatogenesis and causes infertility by impairing committed

Development (2022) 149, dev200205. doi:10.1242/dev.200205

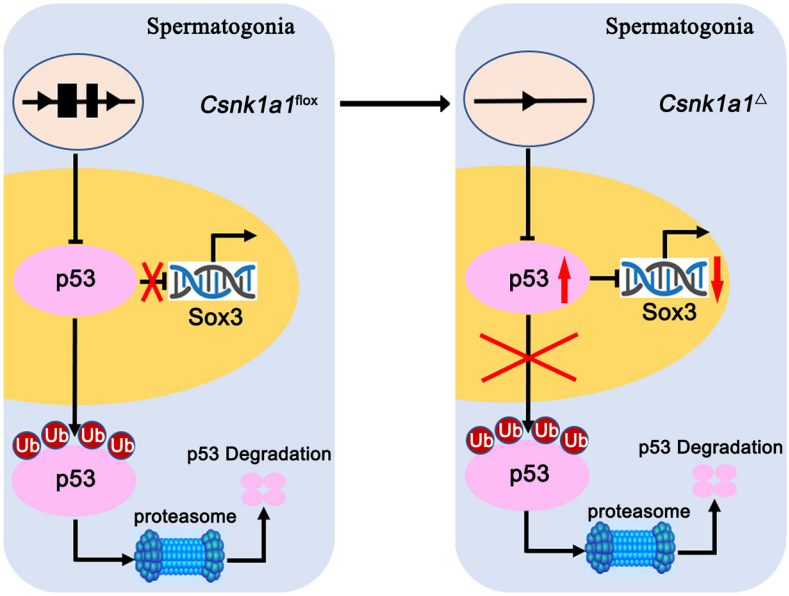

Fig. 8. Schematic summary of CK1α ablation-induced p53-dependent negative regulation of the *Sox3* signaling pathway in mouse spermatogonia. CK1α conditional knockout increases p53 protein and decreases Sox3 protein levels. p53 protein fails to be degraded and accumulates in the spermatogonia nucleus. p53 protein binding to the Sox3 gene promoter leads to failure of Sox3 transcription activation. This affects the maintenance of committed progenitor spermatogonia.

progenitor spermatogonia, although CK1α is expressed in multiple cell types of mouse testis, including spermatogonia, P/D spermatocytes, spermatids and somatic cells, which is coincident with the high expression level of CK1α in testis reported earlier (Jiang et al., 2018). It has been well documented that the maintenance of committed progenitor spermatogonia is a crucial step in determining the success of spermatogenesis (Song and Wilkinson, 2014), and its defect leads to a massive accumulation of SSCs, which ultimately causes the failure of spermatogenesis (Suzuki et al., 2021). In support, our results show that CK1α deletion sharply reduces $Sox3^{+}$ committed progenitor cells and SSCs accumulate on the basement membrane of the seminiferous tubules over time. In addition, it is in consistent with our study in committed progenitor spermatogonia that CK1α is also essential for the maintenance of epidermis progenitor cell status (Bao et al., 2017), and suggests that CK1α plays roles in different types of progenitor cells.

In addition, the results of this study show that CK1α deletion leads to the failure of meiosis initiation due to the defective committed progenitor spermatogonia. It is well known that CK1α is involved in regulating cell division by affecting the mitosis and meiosis (Brockman et al., 1992; Fulcher et al., 2019; Fulcher and Sapkota, 2020; Huo et al., 2022). There are reports that CK1α is essential for the meiosis of female germ cells by affecting the chromosome alignment and segregation (Gross et al., 1997; Wang et al., 2013). However, CK1α deletion causes the loss of spermatocytes, and this prevents us from further detecting the function of CK1α in the meiosis of male germ cells. It is thus important to identify the functions of CK1α in spermatocytes in future studies because CK1α is expressed in P/D spermatocytes, as shown in this study.

Furthermore, the present study has proved that CK1α regulates the maintenance of committed progenitor spermatogonia through the MDM2/p53 signaling pathway. Our data show that CK1α interacts with p53 and that CK1α deletion causes the accumulation of p53 protein and its translocation into the nucleus of spermatogonia. Consistent with our results, previous studies demonstrate that CK1α loss is accompanied with p53 protein activation in epithelium or keratinocytes (Elyada et al., 2011; Chang et al., 2017) and p53 signaling is the most common pathway regulated by CK1α (Huart et al., 2009; Cheong and Virshup, 2011). In addition, p53 signaling is involved in various biological processes, including regulating progenitor cellular homeostasis (McConnell et al., 2016; Zhou et al., 2021), cellular apoptosis and surveillance (Jain and Barton, 2018). However, there is a report that p53 knockout increases the number of progenitor cells in the mouse testis and suggests that p53 is indispensable for negatively regulating the maintenance of committed progenitor spermatogonia (Xiong et al., 2015). Our rescue experiments demonstrate that Sox3-labeled committed progenitor spermatogonia were partially recovered after p53 inhibition in cKO mouse testes, which further confirms that p53 acts downstream of CK1α in the maintenance of committed progenitor spermatogonia.

Finally, the present study demonstrates that CK1α regulates spermatogenesis by p53-Sox3 signaling. The expression and function of the transcription factor Sox3 have been identified in nervous system and reproductive system (Kamachi and Kondoh, 2013; Song and Wilkinson, 2014). In testes, Sox3 promotes the generation of committed progenitor spermatogonia to stimulate spermatogenesis (Raverot et al., 2005), and CK1α positively regulates *Sox3* expression through Sohlh1 and Sohlh2 (Ballow et al., 2006; Toyoda et al., 2009). Although our results here demonstrate that CK1α deletion leads to the accumulation of $Gfr\alpha1^{+}$ SSCs as well as to a decrease in committed progenitors, this is in consistent with the phenotype of Sox3 null testes (McAninch et al., 2020a). Furthermore, by binding the promoter of *Sox3*, our dual-luciferase reporter and ChIP assays prove that *Sox3* is negatively regulated by p53. These results suggest that CK1α-p53 signal affects the maintenance of committed progenitor spermatogonia by targeting *Sox3*.

In conclusion, our data demonstrate a novel mechanism regulating the maintenance of committed progenitor spermatogonia that involves CK1α as well as the p53/Sox3 signaling pathway. CK1α conditional deletion in mouse spermatogonia causes the decrease of $Sox3^{+}$ spermatogonia and p53 protein accumulation, which subsequently result in germ cell defects and male infertility. These are crucial for our understanding the regulating mechanisms of spermatogenesis, although the detailed mechanisms need to be elucidated further.

Development (2022) 149, dev200205. doi:10.1242/dev.200205

MATERIALS AND METHODS

Mice

All animal experimental operations were carried out in accordance with the protocols allowed by the Institutional Animal Care and Use Committee of Yangzhou University. *Csnk1a1*$^{flox/flox}$ mice (Elyada et al., 2011) and *Stra8-Cre* (Sadate-Ngatchou et al., 2008) mice were obtained from The Jackson Laboratory and crossed to obtain *Csnk1a1*$^{fl/\Delta}$*;SCre*$^{+}$ males. The *Csnk1a1*$^{\Delta/+}$*;SCre*$^{+}$ mice were used as controls. All mice were maintained in the C57BL/6 and 129/SvEv mixed background. Genotyping was performed by PCR using mouse tail DNA. PCR primer sequences are listed in Table S2.

Real-time PCR

Mouse testes or cultured SSCs RNAs were isolated using TRIzol reagent (TaKaRa) according to the manufacturer's instructions. Complementary DNA (cDNA) was reverse transcribed from RNA using M-MLV reverse transcription reagents (Promega). Real-time PCR was measured using SYBR Green Core PCR Reagents (Vazyme) in the ABI StepOnePlus Sequence Detection System. Results were analyzed using the delta-delta Ct method and normalized to glyceraldehyde 3-phosphate dehydrogenase (*Gapdh*). Real-time PCR primer sequences are listed in Table S3.

Western blot

Proteins from mouse testes or cultured cells were manually homogenized with radio-immunoprecipitation assay buffer [RIPA, Cell Signaling Technology (CST)] adding 1 mM protease inhibitor phenylmethylsulfonyl fluoride (PMSF, CST). Bicinchoninic acid assay reagent (Beyotime Biotechnology) was applied to detect protein concentrations. The primary and secondary antibodies are listed in Table S20. Quantification of each protein was analyzed by Quantity One software (Bio-Rad) and normalized to α-tubulin.

Immunostaining and histology

Mouse testes were fixed in 4% paraformaldehyde (4% PFA) in phosphate-buffered saline (PBS) overnight at 4°C, then dehydrated, embedded in paraffin wax and sectioned (5 µm). For immunostaining, sections were deparaffinized and antigen retrieval was carried out for 20 min in 0.01 M sodium citrate buffer (pH 6.0). Sections were blocked in 5-10% normal donkey or goat serum for 1-2 h at room temperature (25°C) and stained with primary and secondary antibodies listed in Table S20 and with DAPI.

For Hematoxylin and Eosin staining, paraffin sections were immersed in Hematoxylin solution for 1 min, turned blue in tap water, then immersed in Eosin solution for 30 s, further dehydrated in up to 100% ethanol and xylene, and sealed with neutral resin.

TUNEL assay and caspase 3 immunohistochemistry

TUNEL assays were performed according to the manufacturer's protocol (Promega). Briefly, slides were deparaffinized and then washed from 100% to 50% ethanol and PBS for 5 min each. The slides were fixed in 4% PFA for 20 min and then treated with proteinase K (20 µg/ml) for 30 min for permeabilization. Sections were then incubated with TUNEL reaction mixture for 60 min at 37°C.

For caspase 3 immunohistochemical analysis, the sections were treated with H_2O_2 for 10 min, blocked with 10% NDS for 30 min at room temperature, and incubated with rabbit anti-caspase 3 overnight at 4°C after antigens were retrieved. The sections were then incubated for 1 h with horseradish peroxidase goat anti-rabbit antibody. All sections were visualized by using diaminobenzidine-H_2O_2 and were counterstained with Hematoxylin.

RNA-seq analysis

P7 control and cKO mouse testes RNAs were isolated. RNA isolation, library construction and sequencing were performed on a BGISEQ-500 (Beijing Genomic Institution, www.genomics.org.cn). For the gene expression analysis, the differential expression genes were defined by the bioinformatics service of BGI according to the combination of the absolute value of log2-Ratio ≥1 and Qvalue ≤0.001. In this project, the average comparison rate of the sample compared with the genome was 94.63%, the average comparison rate of the compared gene set was 70.82% and a total of 18,776 genes were detected. All original sequence datasets can be found in the NCBI SRA database under accession numbers SRR14614151, SRR14614152, SRR14614153, SRR14614154, SRR14614155 and SRR14614156.

Isolation of SSCs from postnatal mice

The SSC enriching method has been described previously (Wei et al., 2018). Briefly, after freshly dissected mouse testes were harvested from P7 C57BL/6 pups, a single-cell suspension was formed using 0.125% trypsin (Sigma) and 1 mg/ml collagenase IV (Sigma) for 10 min followed by 5 mg/ml of DNase I (Sigma) for 5-10 min at 37°C. Fetal bovine serum (FBS, 10%) was then added to neutralize. Cell pellets were centrifuged, resuspended and filtered with 40 µm nylon cell strainer. The THY1^{+} SSCs were enriched through CD90.2 MicroBeads (MiltenyiBiotec) and magnetic-activated cell sorting (MiltenyiBiotec), and cultured in 24-well plates with mouse embryonic fibroblasts (MEFs), which were inactivated using mitomycin C in a mixture of 5% CO_2 and 95% air at 37°C.

Mouse SSC and MEF culture

The SSC culture system was established previously (Wei et al., 2018) and employs a CF-1 MEF feeder layer treated with mitomycin C. The culture medium of MEF cells contains Dulbecco's modified Eagle's medium (DMEM), 1× glutamine (Gibco), 1× penicillin/streptomycin (Gibco) and 10% FBS (ThermoFisher).

SSCs were maintained in StemPro-34 SFM (Gibco) containing 1% FBS, N-2 Supplement (Gibco), 15 ng/ml glial cell derived neurotrophic factor (GDNF, Peprotech), 5 mg/ml bovine serum albumin (Sigma), 1 mM sodium pyruvate (Gibco), 10 ng/ml fibroblast growth factor 2 (Peprotech), 2 mM glutamine, 10 mg/ml biotin (Sigma), 20 mg/ml insulin (Sigma), 1× MEM vitamin solution (Gibco), 6 mg/ml D-(+)-glucose (Sigma), 50 mM 2-mercaptoethanol, 1 µl/ml sodium DL-lactate (Sigma), 50 mM 2-mercaptoethanol, 60 ng/ml progesterone (MCE), 30 ng/ml β-estradiol (MCE) and 1× MEM nonessential amino acids solution (NEAA, Gibco).

CK1α and p53 inhibition studies

D4476, an inhibitor of CK1α, was purchased from (MCE, MedChemExpress). D4476 was diluted to 50 mM with DMSO. PFTα (pifithrin α), a p53 inhibitor, was purchased from MCE. PFTα was diluted to 10 mM with DMSO. The CK1α and p53 inhibition study *in vitro* was performed by adding 50 µM D4476 for 24 h and/or 10 µM PFT-α for 1 h to the SSC culture media. *In vivo*, 2.2 mg/kg PFTα was administered by intraperitoneal injection every 24 h from P3 to P7 after *Stra8-cre* activation, and the testes tissues were harvested for RNA and protein assays.

Co-immunoprecipitation

Cultured wild-type mouse undifferentiated spermatogonia were collected in ice-cold RIPA buffer. Protein A/G agarose beads (Santa Cruz) were used to perform all co-immunoprecipitation experiments. Western blot was then performed. In brief, 500 µg cell lysate was incubated with 2 µg anti-CK1α or anti-IgG antibody for 1 h. 20 µl protein A/G PLUS-agarose beads were then added to cell lysate overnight at 4°C. Before performing the western blot, beads were washed five times with PBS.

In situ hybridization

The expressions of Sohlh1 and Sohlh2 were detected by *in situ* hybridization with digoxigenin (DIG)-labeled probes on frozen testis sections. The slides were fixed in fresh 4% DEPC-PFA for 10 min, washed three times for 10 min each in 1×DEPC-PBS, pretreated with 10 µg/ml proteinase K and then washed again in 1×DEPC-PBS. After a 10 min acetylation, pre-hybridization was performed on the slides for 4 h at room temperature, and Sohlh1 and Sohlh2 hybridization was then carried out at 65°C for 16 h. The sections were treated with an alkaline phosphatase (AP)-conjugated antibody to digoxigenin at 4°C overnight after washing with 5×SSC, 0.2×SSC and blocking. The slides were washed and then incubated in nitro tetrazolium blue chloride (NBT) and 5-bromo-4-chloro-3-indolylphosphate p-toluidine salt (BCIP) at room temperature for staining.

Development (2022) 149, dev200205. doi:10.1242/dev.200205

Dual-luciferase reporter assay

The mouse *Sox3*, *Ngn3*, *Sohlh1* and *Sohlh2* promoter luciferase reporter genes were constructed into the pGL3.0 luciferase reporter vector (Promega). The *p53* CDS fragment was amplified to insert into the pcDNA3.1-HYGRO vector containing the BmaHI–NotI restriction sites. Next, *Sox3*, *Ngn3*, *Sohlh1* and *Sohlh2* luciferase reporter vectors, a *p53* expression vector and a pTK-Renilla vector were transfected into human 293FT cells using Lipofectamine 2000 reagent for 24 h and then harvested. Luciferase activities were assayed using Luc-Pair Duo-Luciferase HS Assay Kit (GeneCopoeia). Luciferase activities were normalized to Renilla luciferase activities. These assays were carried out independently three times. The primer sequences are listed in Table S17.

Chromatin immunoprecipitation (ChIP) assay

Chromatin was extracted from the P7 testes of control and cKO mice prepared with the SimpleChIP Plus Enzymatic Chromatin IP Kit (CST). Briefly, testes tissues were dissected and digested. The cell suspension was crosslinked with 1% formaldehyde (Sigma). Chromatin was sheared to 150-500 bp length by sonication. Immunoprecipitation was performed using a p53 antibody. PCR and real-time PCR were performed on control and cKO crosslinked chromatin using primers corresponding to the regions 1-4. We repeated ChIP reactions three times. The primer sequences are listed in Table S18.

Statistical analysis

All statistical analyses of real-time PCR and imaging were performed using at least three independent replicates. Results were expressed as mean±s.e.m. All statistical analyses were performed using Prism 8 (Graphpad Software) and normality (Shapiro–Wilk test) and variance were assessed where appropriate. An unpaired two-tailed Student's *t*-test was performed for two-group comparisons. For making multiple comparisons, one-way ANOVA followed by Tukey's multiple comparisons test or Dunnett's T3 multiple comparisons test was performed. $P<0.05$ was considered to be statistically significant.

Competing interests

The authors declare no competing or financial interests.

Author contributions

Conceptualization: C.L.; Methodology: C.L., D.Z.; Software: D.Z., J.Q.; Validation: K.G.; Formal analysis: C.L.; Investigation: D.Z., L.L.; Resources: D.Z., J.Z.; Data curation: C.L.; Writing - original draft: C.L.; Writing - review & editing: D.Z.; Supervision: S.C.; Project administration: S.C.; Funding acquisition: S.C.

Funding

This work is supported by the National Key Research and Development Program of China (2018YFC1003504), by the Priority Academic Program Development of Jiangsu Higher Education Institutions and by the Postgraduate Research and Practice Innovation Program of Jiangsu Province (Yangzhou University, XKYCX18_111).

Data availability

Data for RNA-sequencing of P7 testes from control and cKO males have been deposited in the NCBI SRA database under accession number SRP320857.

References

Agarwal, M. L., Agarwal, A., Taylor, W. R. and Stark, G. R. (1995). p53 controls both the G2/M and the G1 cell cycle checkpoints and mediates reversible growth arrest in human fibroblasts. *Proc. Natl. Acad. Sci. USA* **92**, 8493-8497. doi:10.1073/pnas.92.18.8493

Ballow, D., Meistrich, M. L., Matzuk, M. and Rajkovic, A. (2006). Sohlh1 is essential for spermatogonial differentiation. *Dev. Biol.* **294**, 161-167. doi:10.1016/j.ydbio.2006.02.027

Bao, X., Siprashvili, Z., Zarnegar, B. J., Shenoy, R. M., Rios, E. J., Nady, N., Qu, K., Mah, A., Webster, D. E., Rubin, A. J. et al. (2017). CSNK1a1 regulates PRMT1 to maintain the progenitor state in self-renewing somatic tissue. *Dev. Cell* **43**, 227-239 e5. doi:10.1016/j.devcel.2017.08.021

Beumer, T. L., Roepers-Gajadien, H. L., Gademan, I. S., van Buul, P. P., Gil-Gomez, G., Rutgers, D. H. and de Rooij, D. G. (1998). The role of the tumor suppressor p53 in spermatogenesis. *Cell Death Differ.* **5**, 669-677. doi:10.1038/sj.cdd.4400396

Brockman, J. L., Gross, S. D., Sussman, M. R. and Anderson, R. A. (1992). Cell cycle-dependent localization of casein kinase I to mitotic spindles. *Proc. Natl. Acad. Sci. USA* **89**, 9454-9458. doi:10.1073/pnas.89.20.9454

Chang, C. H., Kuo, C. J., Ito, T., Su, Y. Y., Jiang, S. T., Chiu, M. H., Lin, Y. H., Nist, A., Mernberger, M., Stiewe, T. et al. (2017). CK1α ablation in keratinocytes induces p53-dependent, sunburn-protective skin hyperpigmentation. *Proc. Natl. Acad. Sci. USA* **114**, E8035-E8044. doi:10.1073/pnas.1702763114

Chen, J. (2016). The cell-cycle arrest and apoptotic functions of p53 in tumor initiation and progression. *Cold Spring Harb. Perspect. Med.* **6**, a026104. doi:10.1101/cshperspect.a026104

Cheong, J. K. and Virshup, D. M. (2011). Casein kinase 1: complexity in the family. *Int. J. Biochem. Cell Biol.* **43**, 465-469. doi:10.1016/j.biocel.2010.12.004

Coates, P. J. (2007). p53 and Mdm2: not all cells are equal. *J. Pathol.* **213**, 357-359. doi:10.1002/path.2275

de Rooij, D. G. and Russell, L. D. (2000). All you wanted to know about spermatogonia but were afraid to ask. *J. Androl.* **21**, 776-798.

Elyada, E., Pribluda, A., Goldstein, R. E., Morgenstern, Y., Brachya, G., Cojocaru, G., Snir-Alkalay, I., Burstain, I., Haffner-Krausz, R., Jung, S. et al. (2011). CKIα ablation highlights a critical role for p53 in invasiveness control. *Nature* **470**, 409-413. doi:10.1038/nature09673

Fulcher, L. J. and Sapkota, G. P. (2020). Mitotic kinase anchoring proteins: the navigators of cell division. *Cell Cycle* **19**, 505-524. doi:10.1080/15384101.2020.1728014

Fulcher, L. J., He, Z., Mei, L., Macartney, T. J., Wood, N. T., Prescott, A. R., Whigham, A. J., Varghese, J., Gourlay, R., Ball, G. et al. (2019). FAM83D directs protein kinase CK1α to the mitotic spindle for proper spindle positioning. *EMBO Rep.* **20**, e47495. doi:10.15252/embr.201847495

Gross, S. D., Simerly, C., Schatten, G. and Anderson, R. A. (1997). A casein kinase I isoform is required for proper cell cycle progression in the fertilized mouse oocyte. *J. Cell Sci.* **110**, 3083-3090. doi:10.1242/jcs.110.24.3083

Hermann, B. P., Mutoji, K. N., Velte, E. K., Ko, D., Oatley, J. M., Geyer, C. B. and McCarrey, J. R. (2015). Transcriptional and translational heterogeneity among neonatal mouse spermatogonia. *Biol. Reprod.* **92**, 54. doi:10.1095/biolreprod.114.125757

Huart, A. S., MacLaine, N. J., Meek, D. W. and Hupp, T. R. (2009). CK1α plays a central role in mediating MDM2 control of p53 and E2F-1 protein stability. *J. Biol. Chem.* **284**, 32384-32394. doi:10.1074/jbc.M109.052647

Huart, A. S., MacLaine, N. J., Narayan, V. and Hupp, T. R. (2012). Exploiting the MDM2-CK1α protein-protein interface to develop novel biologics that induce UBL-kinase-modification and inhibit cell growth. *PLoS One* **7**, e43391. doi:10.1371/journal.pone.0043391

Huo, S., Chen, Z., Li, S., Wang, J., Ma, J., Yang, Y., Zhaxi, Y., Zhao, Y., Zhang, D. and Long, R. (2022). A comparative transcriptome and proteomics study of post-partum ovarian cycle arrest in yaks (Bos grunniens). *Reprod. Domest. Anim.* **57**, 292-303. doi:10.1111/rda.14059

Jain, A. K. and Barton, M. C. (2018). p53: emerging roles in stem cells, development and beyond. *Development* **145**, dev158360. doi:10.1242/dev.158360

Jiang, S., Zhang, M., Sun, J. and Yang, X. (2018). Casein kinase 1α: biological mechanisms and theranostic potential. *Cell Commun. Signal* **16**, 23. doi:10.1186/s12964-018-0236-z

Kamachi, Y. and Kondoh, H. (2013). Sox proteins: regulators of cell fate specification and differentiation. *Development* **140**, 4129-4144. doi:10.1242/dev.091793

Kanatsu-Shinohara, M. and Shinohara, T. (2013). Spermatogonial stem cell self-renewal and development. *Annu. Rev. Cell Dev. Biol.* **29**, 163-187. doi:10.1146/annurev-cellbio-101512-122353

Kaucher, A. V., Oatley, M. J. and Oatley, J. M. (2012). NEUROG3 is a critical downstream effector for STAT3-regulated differentiation of mammalian stem and progenitor spermatogonia. *Biol. Reprod.* **86**, 1-11. doi:10.1095/biolreprod.111.097386

Knippschild, U., Gocht, A., Wolff, S., Huber, N., Lohler, J. and Stöter, M. (2005a). The casein kinase 1 family: participation in multiple cellular processes in eukaryotes. *Cell. Signal.* **17**, 675-689. doi:10.1016/j.cellsig.2004.12.011

Knippschild, U., Wolff, S., Giamas, G., Brockschmidt, C., Wittau, M., Wurl, P. U., Eismann, T. and Stöter, M. (2005b). The role of the casein kinase 1 (CK1) family in different signaling pathways linked to cancer development. *Onkologie* **28**, 508-514. doi:10.1159/000087137

La, H. M. and Hobbs, R. M. (2019). Mechanisms regulating mammalian spermatogenesis and fertility recovery following germ cell depletion. *Cell. Mol. Life Sci.* **76**, 4071-4102. doi:10.1007/s00018-019-03201-6

Mäkelä, J. A. and Hobbs, R. M. (2019). Molecular regulation of spermatogonial stem cell renewal and differentiation. *Reproduction* **158**, R169-R187. doi:10.1530/REP-18-0476

McAninch, D., Thomson, E. P. and Thomas, P. Q. (2020a). Genome-wide DNA-binding profile of SRY-box transcription factor 3 (SOX3) in mouse testes. *Reprod. Fertil. Dev.* **32**, 1260-1270. doi:10.1071/RD20108

McAninch, D., Makela, J. A., La, H. M., Hughes, J. N., Lovell-Badge, R., Hobbs, R. M. and Thomas, P. Q. (2020b). SOX3 promotes generation of

committed spermatogonia in postnatal mouse testes. *Sci. Rep.* **10**, 6751. doi:10.1038/s41598-020-63290-3

McConnell, A. M., Yao, C., Yeckes, A. R., Wang, Y., Selvaggio, A. S., Tang, J., Kirsch, D. G. and Stripp, B. R. (2016). p53 regulates progenitor cell quiescence and differentiation in the airway. *Cell Rep.* **17**, 2173-2182. doi:10.1016/j.celrep.2016.11.007

Molchadsky, A., Rivlin, N., Brosh, R., Rotter, V. and Sarig, R. (2010). p53 is balancing development, differentiation and de-differentiation to assure cancer prevention. *Carcinogenesis* **31**, 1501-1508. doi:10.1093/carcin/bgq101

Nakagawa, T., Sharma, M., Nabeshima, Y., Braun, R. E. and Yoshida, S. (2010). Functional hierarchy and reversibility within the murine spermatogenic stem cell compartment. *Science* **328**, 62-67. doi:10.1126/science.1182868

Oakberg, E. F. (1971). Spermatogonial stem-cell renewal in the mouse. *Anat. Rec.* **169**, 515-531. doi:10.1002/ar.1091690305

Phillips, B. T., Gassei, K. and Orwig, K. E. (2010). Spermatogonial stem cell regulation and spermatogenesis. *Philos. Trans. R. Soc. Lond. Ser. B Biol. Sci.* **365**, 1663-1678. doi:10.1098/rstb.2010.0026

Raverot, G., Weiss, J., Park, S. Y., Hurley, L. and Jameson, J. L. (2005). Sox3 expression in undifferentiated spermatogonia is required for the progression of spermatogenesis. *Dev. Biol.* **283**, 215-225. doi:10.1016/j.ydbio.2005.04.013

Sadate-Ngatchou, P. I., Payne, C. J., Dearth, A. T. and Braun, R. E. (2008). Cre recombinase activity specific to postnatal, premeiotic male germ cells in transgenic mice. *Genesis* **46**, 738-742. doi:10.1002/dvg.20437

Song, H.-W. and Wilkinson, M. F. (2014). Transcriptional control of spermatogonial maintenance and differentiation. *Semin. Cell Dev. Biol.* **30**, 14-26. doi:10.1016/j.semcdb.2014.02.005

Suzuki, H., Sada, A., Yoshida, S. and Saga, Y. (2009). The heterogeneity of spermatogonia is revealed by their topology and expression of marker proteins including the germ cell-specific proteins Nanos2 and Nanos3. *Dev. Biol.* **336**, 222-231. doi:10.1016/j.ydbio.2009.10.002

Suzuki, H., Ahn, H. W., Chu, T., Bowden, W., Gassei, K., Orwig, K. and Rajkovic, A. (2012). SOHLH1 and SOHLH2 coordinate spermatogonial differentiation. *Dev. Biol.* **361**, 301-312. doi:10.1016/j.ydbio.2011.10.027

Suzuki, S., McCarrey, J. R. and Hermann, B. P. (2021). An mTORC1-dependent switch orchestrates the transition between mouse spermatogonial stem cells and clones of progenitor spermatogonia. *Cell Rep.* **34**, 108752. doi:10.1016/j.celrep.2021.108752

Tegelenbosch, R. A. J. and de Rooij, D. G. (1993). A quantitative study of spermatogonial multiplication and stem cell renewal in the C3H/101 F1 hybrid mouse. *Mutat. Res.* **290**, 193-200. doi:10.1016/0027-5107(93)90159-D

Tokue, M., Ikami, K., Mizuno, S., Takagi, C., Miyagi, A., Takada, R., Noda, C., Kitadate, Y., Hara, K., Mizuguchi, H. et al. (2017). SHISA6 confers resistance to differentiation-promoting Wnt/β-catenin signaling in mouse spermatogenic stem cells. *Stem Cell Rep.* **8**, 561-575. doi:10.1016/j.stemcr.2017.01.006

Toyoda, S., Miyazaki, T., Miyazaki, S., Yoshimura, T., Yamamoto, M., Tashiro, F., Yamato, E. and Miyazaki, J. (2009). Sohlh2 affects differentiation of KIT positive oocytes and spermatogonia. *Dev. Biol.* **325**, 238-248. doi:10.1016/j.ydbio.2008.10.019

Wang, L., Lu, A., Zhou, H. X., Sun, R., Zhao, J., Zhou, C. J., Shen, J. P., Wu, S. N. and Liang, C. G. (2013). Casein kinase 1 alpha regulates chromosome congression and separation during mouse oocyte meiotic maturation and early embryo development. *PLoS One* **8**, e63173. doi:10.1371/journal.pone.0063173

Wang, S., Wang, X., Ma, L., Lin, X., Zhang, D., Li, Z., Wu, Y., Zheng, C., Feng, X., Liao, S. et al. (2016). Retinoic acid is sufficient for the in vitro induction of mouse spermatocytes. *Stem Cell Rep.* **7**, 80-94. doi:10.1016/j.stemcr.2016.05.013

Wei, X., Wu, S., Song, T., Chen, L., Gao, M., Borcherds, W., Daughdrill, G. W. and Chen, J. (2016). Secondary interaction between MDMX and p53 core domain inhibits p53 DNA binding. *Proc. Natl. Acad. Sci. USA* **113**, E2558-E2563. doi:10.1073/pnas.1603838113

Wei, C., Lin, H. and Cui, S. (2018). The forkhead transcription factor FOXC2 is required for maintaining murine spermatogonial stem cells. *Stem Cells Dev.* **27**, 624-636. doi:10.1089/scd.2017.0233

Williams, A. B. and Schumacher, B. (2016). p53 in the DNA-damage-repair process. *Cold Spring Harb. Perspect. Med.* **6**, a026070. doi:10.1101/cshperspect.a026070

Xiong, M., Ferder, I. C., Ohguchi, Y. and Wang, N. (2015). Quantitative analysis of male germline stem cell differentiation reveals a role for the p53-mTORC1 pathway in spermatogonial maintenance. *Cell Cycle* **14**, 2905-2913. doi:10.1080/15384101.2015.1069928

Zhou, Q., Nie, R., Li, Y., Friel, P., Mitchell, D., Hess, R. A., Small, C. and Griswold, M. D. (2008). Expression of stimulated by retinoic acid gene 8 (Stra8) in spermatogenic cells induced by retinoic acid: an in vivo study in vitamin A-sufficient postnatal murine testes. *Biol. Reprod.* **79**, 35-42. doi:10.1095/biolreprod.107.066795

Zhou, X., Beilter, A., Xu, Z., Gao, R., Xiong, S., Paulucci-Holthauzen, A., Lozano, G., de Crombrugghe, B. and Gorlick, R. (2021). Wnt/ß-catenin-mediated p53 suppression is indispensable for osteogenesis of mesenchymal progenitor cells. *Cell Death Dis.* **12**, 521. doi:10.1038/s41419-021-03758-w